

Insertions of Small Molecules CO, CH₃NC, SO₂, and CS₂ into the Pd-Pd σ -Bond of Pd₂Cl₂(PMe₂CH₂PMe₂)₂. Crystal and Molecular Structure of Pd₂(μ -CO)Cl₂(PMe₂CH₂PMe₂)₂

Marc L. Kullberg and Clifford P. Kubiak*

Received April 22, 1985

The reaction of Pd₂Cl₂(dmpm)₂ (**1**) with the small molecules CO, CH₃NC, SO₂, and CS₂ leads to insertion into the Pd-Pd bond of **1** and formation of Pd₂(μ -L)Cl₂(dmpm)₂ (L = CO, CH₃NC, SO₂, CS₂). The crystal and molecular structure of the μ -CO complex Pd₂(μ -CO)Cl₂(dmpm)₂ (**2**) has been determined. Complex **2** crystallizes in the orthorhombic space group *P*2₁2₁2₁ with *a* = 15.511 (2) Å, *b* = 11.107 (2) Å, *c* = 12.346 (2) Å, *V* = 2127 (2) Å³, and *Z* = 4. The structure of **2** was refined to convergence leading to *R* and *R*_w of 0.040 and 0.059, respectively, for 1807 observations in the range 6° < 2 θ < 54° with *I* > 2.0 σ (*I*). The Pd-Pd separation is 3.171 (1) Å. Reactions of **2** with SO₂, CH₃NC, and CS₂ proceed with facile displacement of the bridging carbonyl to form respectively the μ -SO₂ (**3**), μ -CH₃NC (**5**), and μ -CS₂ (**4**) complexes. Reaction with at least 3 equiv of CH₃NC leads to displacement of the terminal chlorides and formation of [Pd₂(μ -CH₃NC)(CH₃NC)₂](dmpm)₂[Cl]₂ (**6**). The three isocyanide ligands of **6** are observed by ¹H NMR to be equivalent at 25 °C. At -80 °C both terminal and bridging isocyanide resonances are evident in a 2:1 ratio. The ³¹P{¹H} NMR chemical shifts of complexes **2-5** qualitatively follow the electrophilicity of the added small molecule in the order SO₂ > CO > CH₃NC > CS₂.

Over the past several years, the insertion of small molecules into the M-M bonds of diphosphine-bridged binuclear complexes has been an area of considerable interest.³⁻¹⁵ These studies have sought to elucidate the chemical nature of the M-M interaction in the case of two metal atoms. The bridging diphosphine ligands also generally preserve the binuclear structures of these complexes. Most of the work to date in the area of diphosphine-supported M-M bonds has involved the ligand bis(diphenylphosphino)methane (dppm).²⁵ Recently, we^{3,13-14} and others¹⁷⁻²² have initiated studies of binuclear complexes bridged by the diphosphine bis(dimethylphosphino)methane (dmpm). The reactivity of the M-M bonds of these complexes is expected to be enhanced by the greater

donor ability and smaller steric requirements of dmpm. The dmpm-bridged palladium complexes Pd₂X₂(dmpm)₂ (X = Cl, Br, OH) have also been found to be highly soluble in water,^{3,13,14} in which they retain their binuclear structures. The water solubility of these complexes holds promise in facilitating the phase separation of the products and catalysts of homogeneously catalyzed reactions. We report herein the synthesis of complexes Pd₂Cl₂(μ -L)(dmpm)₂ (L = CO, CH₃NC, SO₂, CS₂), by addition of small molecules, L, to Pd₂Cl₂(dmpm)₂. The new complexes have been completely characterized by IR, ¹H, ¹³C{¹H}, and ³¹P{¹H} NMR, and UV-vis spectroscopy. The crystal and molecular structure of the μ -CO complex, Pd₂(μ -CO)Cl₂(dmpm)₂ is also reported.

Experimental Section

Materials. All solvents were deoxygenated prior to use. CS₂ and anhydrous diethyl ether (Mallinckrodt) were used without further purification. Acetonitrile and methylene chloride were freshly distilled from 3A molecular sieves and CaH₂, respectively, under N₂. CO and SO₂ were used as received from Matheson Gas, Inc. A generous loan of PdCl₂ was obtained from Johnson Matthey, Inc.

[Pd(CO)Cl]_n was prepared according to the procedure of Schnabel and Kober.¹ Methyl isocyanide was prepared by the dehydration of *N*-methylformamide following the procedure of Werner et al.² The ligand bis(dimethylphosphino)methane was prepared as reported previously.¹⁴

Physical Measurements. Elemental analyses were performed by Dr. H. D. Lee of the Microanalytical Laboratory, Department of Chemistry, Purdue University. UV-vis spectra were recorded on a Hewlett Packard 8450A diode array spectrophotometer. Infrared spectra were recorded on a Perkin-Elmer 700 instrument for 4000-600 cm⁻¹ and on a Digi-Lab FTS-20B instrument for 100-400 cm⁻¹. ¹H, ³¹P{¹H}, and ¹³C{¹H} NMR spectra were recorded on a Varian XL-200 spectrophotometer. ¹H and ¹³C{¹H} NMR were measured against internal Me₄Si and ³¹P{¹H} NMR against external 85% H₃PO₄.

Synthesis of Pd₂Cl₂(dmpm)₂ (1**).** This complex was prepared as previously reported.^{3,14}

Synthesis of Pd₂(μ -CO)Cl₂(dmpm)₂ (2**).** A solution of 0.10 g (0.18 mmol) of **1** in 10 mL of CH₃CN was prepared. To this solution was added CO, and the system was stirred for 1 h. The volume of the solution was then reduced at which time an orange-yellow crystalline solid precipitated from solution. The solution was cooled to -10 °C, and the crystals were collected. Further precipitation was effected by layering diethyl ether over the CH₃CN solution and cooling to -10 °C. Total yield: 0.072 g (0.12 mmol, 68%). X-ray quality crystals were obtained by preparing a 0.02 M solution of **1** in CH₃CN, charging the system with CO, and allowing the solution to sit at room temperature for ca. 10 h. The density of the crystals was determined by the flotation method using CCl₄/CHBr₃ and was found to be 1.81 (1) g/cm³. IR (CH₂Cl₂): ν (CO) = 1710 cm⁻¹. IR (Nujol mull): ν (CO) = 1705 cm⁻¹. ¹H NMR (CD₂Cl₂): δ 1.21 (m, CH₂), 1.61 (m, CH₃), 1.48 (m, CH₃). ¹³C{¹H} NMR (CD₂Cl₂, ¹³CO): δ 244 (q, CO), 41.9 (t, CH₂), 16.9 (q, CH₃), 13.8 (q, CH₃). ³¹P{¹H} NMR (CD₂Cl₂): δ 1.28 (s). Anal. Calcd for

- Schnabel, W.; Kober, E. *J. Organomet. Chem.* **1969**, *19*, 455.
- Cassanova, J.; Schuster, R. E.; Werner, N. D. *J. Chem. Soc.* **1963**, 4280.
- Kullberg, M. L.; Kubiak, C. P. *Organometallics* **1984**, *3*, 632.
- Colton, R.; McCormick, M. J.; Pannan, C. D. *Aust. J. Chem.* **1978**, *31*, 1425.
- Benner, L. S.; Balch, A. L. *J. Am. Chem. Soc.* **1978**, *100*, 6099.
- Rankin, D. W. H.; Robertson, H. E.; Karsch, H. H. *J. Mol. Struct.* **1981**, *77*, 121.
- Balch, A. L.; Benner, L. S.; Olmstead, M. M. *Inorg. Chem.* **1979**, *18*, 2996.
- Holway, R. G.; Penfold, B. R.; Colton, R.; McCormick, M. J. *J. Chem. Soc., Chem. Commun.* **1976**, 485.
- Olmstead, M. M.; Benner, L. S.; Hope, H.; Balch, A. L. *Inorg. Chim. Acta* **1979**, *32*, 193.
- Brown, M. P.; Fisher, J. R.; Puddephatt, R. J.; Seddon, K. R. *Inorg. Chem.* **1979**, *18*, 2808.
- Pringle, P. G.; Shaw, B. L. *J. Chem. Soc., Dalton Trans.* **1983**, 889.
- Cameron, T. S.; Gardner, P. A.; Grundy, K. R. *J. Organomet. Chem.* **1981**, *212*, C19.
- Kullberg, M. L.; Kubiak, C. P. *Mol. Chem.* **1984**, *1*, 171.
- Kullberg, M. L.; Lemke, F. R.; Powell, D. R.; Kubiak, C. P. *Inorg. Chem.* **1985**, *24*, 3589.
- DeLaet, D. L.; Powell, D. R.; Kubiak, C. P. *Organometallics* **1985**, *4*, 954.
- A notable exception to the generally stable binuclear trans-bridging diphosphine structure can be found in: Olmstead, M. M.; Lee, C.; Balch, A. L. *Inorg. Chem.* **1982**, *21*, 2712 and references contained therein.
- King, R. B.; Raghuvver, K. S. *Inorg. Chem.* **1984**, *23*, 2482.
- Ling, S. S. M.; Puddephatt, R. J.; Manojlovic-Muir, L.; Muir, K. W. *Inorg. Chim. Acta* **1983**, *77*, L95.
- Ling, S. S. M.; Puddephatt, R. J.; Manojlovic-Muir, L.; Muir, K. W. *J. Organomet. Chem.* **1983**, *255*, C11.
- Karsch, H. H.; Milewski-Mahrla, B. *Angew. Chem.* **1981**, *93*, 825.
- Karsch, H. H.; Schubert, V. Z. *Naturforsch., B: Anorg. Chem., Org. Chem.* **1982**, *37B*, 186.
- Manojlovic-Muir, L.; Muir, K. W.; Frew, A. A.; Ling, S. S. M.; Thomson, M. A.; Puddephatt, R. J. *Organometallics* **1984**, *3*, 1637.
- Kubiak, C. P.; Eisenberg, R. *J. Am. Chem. Soc.* **1977**, *99*, 6129.
- Olmstead, M. M.; Hope, H.; Benner, L. S.; Balch, A. L. *J. Am. Chem. Soc.* **1977**, *99*, 5502.
- Puddephatt, R. J. *Chem. Soc. Rev.* **1983**, *12*, 99.

$C_{11}H_{28}P_4Cl_2OPd_2$: C, 22.63; H, 4.83; Cl, 12.40. Found: C, 22.75; H, 4.94; Cl, 12.30.

Synthesis of $Pd_2(\mu-SO_2)Cl_2(dmpm)_2$ (3). A solution of 0.052 g (0.09 mmol) of **1** in 1 mL of CH_2Cl_2 was prepared. The system was charged with SO_2 while being stirred. The orange solution became deep red in 3–4 min and was stirred for 1 h under $SO_2(g)$ and then cooled to $-78^\circ C$. Diethyl ether was added slowly to form a layer above the CH_2Cl_2 solution. The solution was placed in a freezer ($-10^\circ C$), and the two layers were allowed to diffuse together. The red crystalline solid which precipitated from solution was filtered, washed with diethyl ether, and dried under vacuum, yielding 0.041 g (0.07 mmol, 71%) of product. IR (Nujol mull): $\nu(SO_2) = 1150, 1030\text{ cm}^{-1}$. $^1H\text{ NMR}$ (CD_2Cl_2) δ 2.34 (m, CH_2), 1.65 (m, CH_3), 1.60 (m, CH_3), 1.43 (m, CH_2), 1.36 (m, CH_2). $^{13}C\{^1H\}$ NMR (CD_2Cl_2): δ 25.74 (t, CH_2), 15.23 (q, CH_3), 13.13 (q, CH_3). $^{31}P\{^1H\}$ NMR (CD_2Cl_2): δ 9.04 (s). Anal. Calcd for $C_{10}H_{28}P_4Cl_2SO_2Pd_2$: C, 19.37; H, 4.52; Cl, 11.44; S, 5.17. Found: C, 19.05; H, 4.66; Cl, 12.21; S, 6.19.

Synthesis of $Pd_2(\mu-CS_2)Cl_2(dmpm)_2$ (4). A solution of 0.098 g (0.18 mmol) of **1** in 5 mL of CH_2Cl_2 was prepared. To this was added 0.1 mL (1.8 mmol) of CS_2 . The solution color immediately changed from orange to an orange-red. The solution was stirred under N_2 for 2 h, and the volume was reduced by one-half, cooled to $-78^\circ C$, and covered with a layer of an equal volume of Et_2O . The solution was then placed in a freezer ($-10^\circ C$) until diffusion of the two layers was complete. Orange-red crystals were collected by filtration yield 0.066 g (0.10 mmol, 60%). IR (Nujol mull): $\nu(CS_2) = 1010\text{ cm}^{-1}$. $^1H\text{ NMR}$ (CD_2Cl_2): δ 2.40 (m, CH_2), 1.71 (m, CH_3), 1.57 (m, CH_3), 1.39 (m, CH_3). $^{13}C\{^1H\}$ NMR (CD_2Cl_2): δ 27.96 (t, CH_2), 12.86 (m, CH_3). $^{31}P\{^1H\}$ NMR (CD_2Cl_2): δ -8.83 (AA'BB'). Anal. Calcd for $C_{11}H_{28}P_4S_2Cl_2Pd_2$: C, 20.91; H, 4.47; Cl, 11.22; S, 10.15. Found: C, 20.91; H, 4.51; Cl, 12.38; S, 11.06.

Synthesis of $Pd_2(\mu-CH_3NC)Cl_2(dmpm)_2$ (5). A solution of 0.105 g (0.19 mmol) of **1** in 5 mL of CH_3CN was prepared. To this was added 11.2 μ L (0.19 mmol) of CH_3NC . The color of the solution rapidly changed from orange to bright yellow. The solution was stirred for 2 h, and its volume was reduced to 2 mL. This solution was then placed in a freezer ($-10^\circ C$) for ca. 10 h and then filtered, yielding a bright yellow solid, yield 0.081 g (0.14 mmol, 74%). IR (CH_2Cl_2): $\nu(CN) = 1680$ (m), 1635 (s) cm^{-1} . IR (Nujol mull): $\nu(CN) = 1675$ (m), 1630 (s) cm^{-1} . $^1H\text{ NMR}$ (CD_2Cl_2): δ 3.28 (s, CH_3NC), 1.58 (m, CH_3), 1.52 (m, CH_3) (dmpm methylene and methyl resonances are overlapped at δ 1.58 and 1.52). $^{13}C\{^1H\}$ NMR (CD_2Cl_2): δ 23.69 (t, CH_2), 13.63 (m, CH_3), -0.46 (s, CH_3NC). $^{31}P\{^1H\}$ NMR (CD_2Cl_2): δ 0.96 (s). Anal. Calcd for $C_{12}H_{31}NP_4Cl_2Pd_2$: C, 24.15; H, 5.23; N, 2.35; Cl, 11.88. Found: C, 23.76; H, 5.44; N, 2.41; Cl, 12.32.

Synthesis of $[Pd_2(\mu-CH_3NC)(CH_3NC)_2(dmpm)_2]Cl_2$ (6). A solution of 0.10 g (0.18 mmol) of **1** in 5 mL of CH_3CN was prepared. To this was added 0.1 mL (1.7 mmol) of CH_3NC . The color of the solution quickly changed from orange to golden yellow. The solution was stirred for 2 h, its volume was reduced to 3 mL, and diethyl ether was added slowly to induce precipitation of the product. The solution was filtered, yielding 0.052 g of a yellow solid (0.077 mmol, 42%). IR (Nujol mull): $\nu(CN) = 2230$ (s), 1670 (w), 1625 (m) cm^{-1} . IR (CH_2Cl_2): $\nu(CN) = 2240$ (s), 2180 (m), 1680 (m), 1640 (s) cm^{-1} . $^1H\text{ NMR}$ (CD_2Cl_2): δ 3.33 (m, br, CH_3NC), 1.62 (m, CH_3) (methylene resonance is obscured by methyl resonances). $^{13}C\{^1H\}$ NMR (CD_2Cl_2): δ 23.51 (t, CH_2), 14.27 (m, CH_3), -0.46 (s, CH_3NC). $^{31}P\{^1H\}$ NMR (CD_2Cl_2): δ 1.96 (s). Anal. Calcd for $C_{16}H_{37}N_3P_4Cl_2Pd_2$: C, 28.28; H, 5.49; N, 6.19; Cl, 10.44. Found: C, 26.92; H, 5.93; N, 5.74; Cl, 10.41.

Crystal Data Collection and Reduction. An orange crystal of **2** was used for determination of cell parameters and subsequent data collection. The crystal was mounted on a glass fiber with epoxy and transferred to the diffractometer. Crystal survey, unit cell dimension determination, and data collection were accomplished on a Enraf-Nonius CAD-4 automated single-crystal diffractometer using Zr-filtered Mo $K\alpha$ radiation ($\lambda = 0.71069\text{ \AA}$) at room temperature. The observed systematic absences of $h00, 0k0$, and $00l$, $h = 2n + 1$, $k = 2n + 1$, and $l = 2n + 1$, are consistent with the orthorhombic space group $P2_12_12_1$. Cell dimensions were determined from a least-squares refinement of intense, high-angle reflections ($29^\circ \leq 2\theta \leq 43^\circ$). Data were collected by using Mo $K\alpha$ radiation in the range $6^\circ \leq 2\theta \leq 54^\circ$. Three standard reflections were monitored every 100 observations, and intensities showed no significant trends over data collection. The linear absorption coefficient for Mo $K\alpha$ radiation is 22.16 cm^{-1} , and an empirical absorption correction based on a series of ψ scans was applied to the data. The final set of data consisted of 2536 unique reflections of which 1807 had $I > 2.0\sigma(I)$.

Solution and Refinement of the Structure. The structure was solved by the MULTAN 11/82 program package and refined by full-matrix least-squares methods in the space group $P2_12_12_1$. All hydrogen atoms were included, but not refined, at calculated positions. Convergence of

Table I. Positional Parameters and Their Estimated Standard Deviations^a

atom	x	y	z	$B, \text{\AA}^2$
Pd1	0.30269 (6)	0.26229 (9)	0.35206 (7)	2.39 (2)
Pd2	0.43554 (6)	0.18601 (9)	0.16926 (7)	2.61 (2)
P1	0.4172 (2)	0.2510 (4)	0.4719 (2)	2.89 (7)
P2	0.1949 (2)	0.2689 (3)	0.2208 (3)	3.06 (7)
P3	0.5419 (2)	0.1527 (3)	0.2993 (3)	2.74 (7)
P4	0.3235 (2)	0.1845 (4)	0.0420 (3)	3.48 (8)
Cl2	0.5360 (2)	0.2893 (5)	0.0477 (3)	5.4 (1)
Cl1	0.2394 (3)	0.4223 (4)	0.4630 (3)	4.84 (9)
C1	0.3481 (9)	0.118 (1)	0.2702 (9)	2.8 (3)
O1	0.3235 (7)	0.0229 (8)	0.2821 (8)	3.9 (2)
C11	0.474 (1)	0.396 (1)	0.484 (1)	4.5 (4)
C12	0.3911 (9)	0.216 (2)	0.612 (1)	4.9 (4)
C13	0.5033 (8)	0.143 (1)	0.441 (1)	3.0 (3)
C21	0.1207 (9)	0.146 (2)	0.225 (1)	4.6 (4)
C22	0.120 (1)	0.397 (2)	0.228 (1)	6.2 (4)
C23	0.2327 (9)	0.280 (1)	0.081 (1)	3.7 (3)
C31	0.625 (1)	0.258 (2)	0.301 (1)	4.8 (4)
C32	0.6010 (9)	0.014 (1)	0.285 (1)	4.1 (3)
C41	0.352 (1)	0.241 (2)	-0.093 (1)	6.2 (5)
C42	0.280 (1)	0.041 (2)	0.017 (1)	5.4 (4)
H11A	0.4309	0.4626	0.5004	5*
H11B	0.5174	0.3935	0.5431	5*
H11C	0.5033	0.4167	0.4137	5*
H12A	0.3423	0.2706	0.6396	5*
H12B	0.3695	0.1303	0.6198	5*
H12C	0.4414	0.2272	0.6614	5*
H12A	0.4822	0.0580	0.4538	5*
H12B	0.5543	0.1570	0.4904	5*
H21A	0.0973	0.1352	0.2998	5*
H21B	0.0708	0.1619	0.1740	5*
H21C	0.1498	0.0697	0.2014	5*
H22A	0.0934	0.4043	0.3007	5*
H22B	0.1511	0.4746	0.2100	5*
H22C	0.0720	0.3873	0.1721	5*
H23A	0.2478	0.3645	0.0663	5*
H23B	0.1820	0.2561	0.0325	5*
H31A	0.6502	0.2707	0.2278	5*
H31B	0.6037	0.3383	0.3297	5*
H31C	0.6732	0.2307	0.3518	5*
H32A	0.6262	0.0074	0.2104	5*
H32B	0.6499	0.0111	0.3392	5*
H32C	0.5624	-0.0567	0.2982	5*
H41A	0.4036	0.1939	-0.1218	5*
H41B	0.3032	0.2307	-0.1442	5*
H41C	0.3689	0.3278	-0.0890	5*
H42A	0.3283	-0.0194	-0.0058	5*
H42B	0.2518	0.0044	0.0824	5*
H42C	0.2372	0.0404	-0.0444	5*

^a B values for anisotropically refined atoms are given in the form of the isotropic equivalent thermal parameter defined as $\frac{1}{3}[a^2B(1,1) + b^2B(2,2) + c^2B(3,3) + ab(\cos \gamma)B(1,2) + ac(\cos \beta)B(1,3) + bc(\cos \alpha)B(2,3)]$. Atoms with starred B values were not refined, but were included in refinements at calculated positions with fixed isotropic temperature factors.

the full-matrix least-squares refinement gave residuals of $R = 0.040$ and $R_w = 0.059$. In all refinements the functions minimized was $\sum w(|F_o| - |F_c|)^2$ where $w = 1/\sigma^2(F)$. All programs used were from the SDP program library, and all calculations were carried out on a PDP 11/34 computer.

Final positional and thermal parameters are listed in Table I. A summary of crystal and intensity collection data can be found in Table II. Complete tables of bond angles, bonding and nonbonding distances, torsion angles, refined temperature factors, and observed and calculated structure factors are available as supplementary material.

Discussion

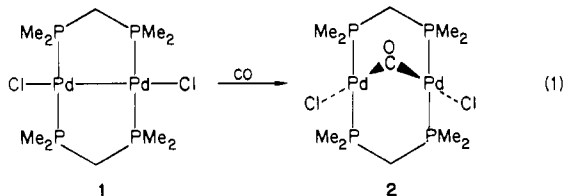
Complex **2** is prepared by the reaction of **1** with CO at room temperature in methylene chloride. Yields of **2** are quantitative as monitored by NMR, and the complex can generally be isolated as an orange crystalline solid in $\sim 70\%$ yield. As a solid, **2** is air-stable. However, in dilute solutions, **2** slowly loses CO, reverting to **1**. The IR spectrum of **2** reveals a strong $\nu(CO)$ band at 1705 cm^{-1} (Nujol). This agrees very well with the spectra of the related *dam*- (bis(diphenylarsino)methane) and *dppm*-bridged

Table II. Summary of Crystal Data and Intensity Collection for $\text{Pd}_2(\mu\text{-CO})\text{Cl}_2(\text{dmpm})_2$

A. Crystal Data	
formula	$\text{Pd}_2\text{Cl}_2(\text{CO})(\text{C}_5\text{H}_{14}\text{P}_2)_2$
fw	583.9
cryst	orange
cell params (errors)	
<i>a</i> , Å	15.511 (2)
<i>b</i> , Å	11.107 (2)
<i>c</i> , Å	12.346 (2)
<i>V</i> , Å ³	2127 (2)
Laue symmetry	orthorhombic
space group	$P2_12_12_1$
<i>Z</i>	4
<i>d</i> _{obsd} , g/cm ³	1.81 (1) (by flotation)
<i>d</i> _{calcd} , g/cm ³	1.80
B. Data Collection and Reduction	
radiation	Zr-filtered, Mo $K\alpha$ ($\lambda = 0.71069$ Å)
diffractometer	CAD-4
temp, °C	25
scan range, deg	$6 < 2\theta < 54$
scan method	ω - 2θ
systematic absences	$h00, h = 2n + 1$ $0k0, k = 2n + 1$ $00l, l = 2n + 1$ (260); (705); (057)
monitor reflns	(260); (705); (057)
scan angle	$1.0 + 0.35(\tan \theta)$
horiz aperture	$4.0 + 0.5(\tan \theta)$
vert aperture, mm	4.0
octant collcd	<i>hkl</i>
no. of unique data	1807 [$I > 2.0\sigma(I)$]
μ , cm ⁻¹	22.159
abs cor	empirical
<i>T</i> _{min} , <i>T</i> _{max}	0.850, 0.999
C. Solution and Refinement	
<i>R</i>	0.040
<i>R</i> _w	0.059
<i>S</i> ^a	2.063
max and mean shift/error	0.07, 0.02
max residual e density	0.599

^a Esd of an observation of unit weight.

complexes: $\text{Pd}_2(\mu\text{-CO})\text{Cl}_2(\text{dam})_2$,⁴ $\nu(\text{CO})$ 1720 cm⁻¹; $\text{Pd}_2(\mu\text{-CO})\text{Cl}_2(\text{dppm})_2$,⁵ $\nu(\text{CO})$ 1705 cm⁻¹. The electronic absorption spectrum of **2** is qualitatively similar to that of **1** with one major exception: **2** is distinguished by an intense new band at 444 nm. All UV-vis data for the new complexes prepared in this study are presented in Table III. The spectroscopic and analytical data pertaining to **2** suggest the complex is the result of CO insertion into the Pd-Pd bond of **1** (eq 1). This notion is confirmed by the crystal and molecular structure determination described below.



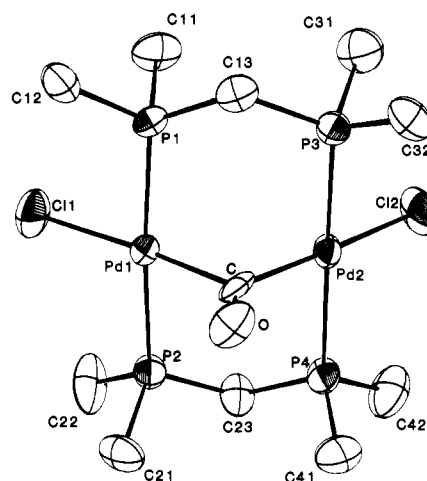
The crystal structure of **2** is composed of discrete $\text{Pd}_2(\mu\text{-CO})\text{Cl}_2(\text{dmpm})_2$ molecules. There are no solvent molecules of crystallization or unusual intermolecular contacts. The molecular structure of **2** consists of two Pd atoms bridged by two mutually trans dmpm ligands and one carbon monoxide ligand. The bridging carbon monoxide is mutually trans to two terminal chloride ligands. The coordination geometry about each Pd center is thus approximately square planar, and overall the molecular structure can be described as typical of the A-frame geometry.^{23,24} An ORTEP drawing of the molecule including all non-hydrogen atoms is presented in Figure 1.

The Pd-Pd separation of 3.171 (1) Å is consistent with no net metal-metal bonding interaction. This value is somewhat shorter than those found in the corresponding dppm- and dam-

Table III. Electronic Spectral Data for $\text{Pd}_2(\mu\text{-X})\text{Cl}_2(\text{dmpm})_2$ Complexes^a

compd	λ_{max} , nm (ϵ , cm ⁻¹ M ⁻¹)
$\text{Pd}_2\text{Cl}_2(\text{dmpm})_2$ (1)	385 (5700), 320 (13 100), 278 (22 100), 243 (10 900)
$\text{Pd}_2(\mu\text{-CO})\text{Cl}_2(\text{dmpm})_2$ (2)	444 (11 730), 383 (6100), 284 (11 140), 241 (18 380)
$\text{Pd}_2(\mu\text{-SO}_2)\text{Cl}_2(\text{dmpm})_2$ (3)	478 (2500), 312 (8130), 230 (16 000)
$\text{Pd}_2(\mu\text{-CS}_2)\text{Cl}_2(\text{dmpm})_2$ (4)	486 (290), 366 (sh, 5800), 332 (sh, 13 900), 314 (17 200), 256 (24 300)
$\text{Pd}_2(\mu\text{-CNCH}_3)\text{Cl}_2(\text{dmpm})_2$ (5)	406 (9360), 366 (sh, 5100), 314 (sh, 5450), 247 (19 400)
$[\text{Pd}_2(\mu\text{-CNCH}_3)(\text{CNCH}_3)_2\text{-}(\text{dmpm})_2][\text{Cl}]_2$ (6)	406 (8200), 366 (sh, 4400), 314 (sh, 4600), 289 (sh, 7600), 245 (19 100)

^a All spectra recorded for CH_2Cl_2 solutions.

**Figure 1.** ORTEP drawing of the $\text{Pd}_2(\mu\text{-CO})\text{Cl}_2(\text{dmpm})_2$ molecule, with 50% probability thermal ellipsoids shown for the non-hydrogen atoms.

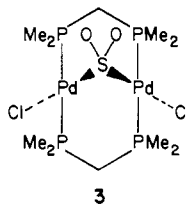
bridged complexes: $\text{Pd}_2(\mu\text{-SO}_2)(\text{dppm})_2$,⁷ 3.30 Å; $\text{Pd}_2(\mu\text{-S})\text{Cl}_2(\text{dppm})_2$,⁷ 3.258 (2) Å; $\text{Pd}_2(\mu\text{-CO})\text{Cl}_2(\text{dam})_2$,⁴ 3.274 (8) Å. The Pd-Pd separation is only slightly longer than the mean adjacent dmpm phosphorus atom nonbonding distance (3.099 Å). The lengthening of the Pd-Pd internuclear distance compared to that in Pd-Pd-bonded species $\text{Pd}_2\text{Br}_2(\text{dmpm})_2$ ¹⁴ has the effect of increasing the P-P nonbonding distance from 2.92 Å³ to 3.099 Å in the present structure. This also has the effect of widening the methylene carbon bond angle from 107.1 (5)° for $\text{Pd}_2\text{Br}_2(\text{dmpm})_2$ ¹⁴ to a mean angle of 115° in **2**, which compares well with that of the free ligand.⁶ These increases in nonbonding distances and bond angles apparently lessen the strain in the eight-membered $\text{Pd}_2\text{P}_4\text{C}_2$ ring compared to the Pd-Pd bonded systems, $\text{Pd}_2\text{Br}_2(\text{dmpm})_2$,³ $\text{Pd}_2\text{Br}_2(\text{dppm})_2$,⁸ and $\text{Pd}_2\text{Cl}(\text{SnCl}_3)(\text{dppm})_2$.⁹ Each of these latter three complexes exhibits a highly twisted $\text{Pd}_2\text{P}_4\text{C}_2$ ring. The twisting is apparently diminished as the Pd-Pd separation increases upon CO insertion.

The bridging carbon monoxide is situated approximately symmetrically between the two Pd centers with Pd1-C1 and Pd2-C1 distances of 2.024 (13) Å and 1.991 (13) Å, respectively. These distances are slightly longer than the mean Pd-C distance in the related $\mu\text{-CO}$ complex, $\text{Pd}_2(\mu\text{-CO})\text{Cl}_2(\text{dam})_2$ (1.90 Å)⁴, and as a consequence the Pd1-C1-Pd2 bond angle of 104.3 (6)° is nearly 15° more acute than in $\text{Pd}_2(\mu\text{-CO})\text{Cl}_2(\text{dam})_2$. The carbonyl Cl-O bond length of 1.130 (20) Å is also significantly shorter than that found in the related $\text{Pd}_2(\mu\text{-CO})\text{Cl}_2(\text{dam})_2$ complex (1.29 (8) Å). The Pd-Cl bond distances of **2**, 2.449 (4), on the other hand are unusually long compared to similar dppm-bridged complexes $\text{Pd}_2(\mu\text{-S})\text{Cl}_2(\text{dppm})_2$ (2.372 (5) Å)⁷ and $\text{Pd}_2(\mu\text{-SO}_2)\text{Cl}_2(\text{dppm})_2$ (2.381 (4) Å)⁷ and dam-bridged complex $\text{Pd}_2(\mu\text{-CO})\text{Cl}_2(\text{dam})_2$ (2.31 (2) Å).⁴ The mean Pd-P bond distance of 2.33 Å however closely agrees with those of related dppm-bridged structures for $\text{Pd}_2(\mu\text{-S})\text{Cl}_2(\text{dppm})_2$ (2.32 Å)⁷ and $\text{Pd}_2(\mu\text{-SO}_2)\text{-}$

$\text{Cl}_2(\text{dppm})_2$ (2.35 Å).⁷ There is nothing unusual about the bridging dmpm ligands. The phosphorus atoms approach tetrahedral geometry as expected. The largest deviations from idealized tetrahedral phosphorus are $\text{C21-P2-C22} = 100.5$ (8)° and $\text{Pd1-P1-C13} = 117.4$ (4)°. The angles P1-C13-P3 and P2-C23-P4 through the dmpm methylene carbon are 113.2 (7)° and 117.1 (8)°, respectively, approximately the same as that for the free ligand,⁶ 115° , in the gas phase.

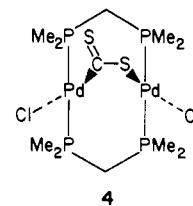
Complex **1** also reacts readily with SO_2 at room temperature. The reaction is essentially quantitative as monitored by NMR. Isolated yields of the red crystalline solid **3** are 70%. Complex **3** is air-stable and stable with respect to SO_2 loss in solution under an N_2 atmosphere, even over periods of months. Thus **2** is easily converted to **3** under an SO_2 atmosphere. The IR spectrum of **3** reveals $\nu(\text{SO}_2) = 1150, 1030 \text{ cm}^{-1}$.

The 200-MHz ^1H NMR spectrum of **3** reveals two well-separated methylene resonances. The lower field signal at $\delta 2.34$ is a complex seven-line multiplet, resulting from overlap of the two halves of an AB doublet of virtual quintets. Virtual coupling of the four phosphorus nuclei in bis(diphosphine)-bridged binuclear complexes is quite common.⁷ The second methylene resonance appears as a doublet of quintets with $^2J_{\text{H}_A\text{H}_B} = 10.5 \text{ Hz}$ and $J_{\text{P-H}} = 2.0 \text{ Hz}$. Qualitatively, the methylene region in the ^1H NMR spectrum of **3** is similar to that of the dppm analogue $\text{Pd}_2(\mu\text{-SO}_2)\text{Cl}_2(\text{dppm})_2$.⁷ The methyl protons of **3** give rise to two separate signals at $\delta 1.65$ and 1.60 , each of which appears as a phosphorus-split virtual quintet. The $^{31}\text{P}\{^1\text{H}\}$ NMR spectrum of **3** shows a singlet at $\delta 9.04$, indicating a single phosphorus environment on the NMR time scale. The electronic absorption spectrum of **3** reveals an intense band, $\lambda_{\text{max}} = 478 \text{ nm}$. On the basis of spectroscopic data observed for **3** and its similarity to that for **2**, the structure of **3** is proposed to be a symmetric $\mu\text{-SO}_2$ adduct.

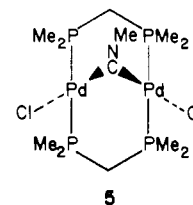


The reaction of **1** with CS_2 proceeds readily and quantitatively at 25°C . A deep red-orange crystalline material, $\text{Pd}_2(\mu\text{-CS}_2)\text{Cl}_2(\text{dmpm})_2$ (**4**), is isolated in 60% yield. The thermodynamic stability of **4** is greater than that for **2**. This is evident from the results of displacement reactions. The reaction of **2** with CS_2 gives **4**, while prolonged exposure of solutions of **4** to CO do not give measurable quantities of **2**. Similar displacement reactions with SO_2 suggest that the relative stabilities of the complexes formed by the reactions of small molecules with **1** follow the order $\text{SO}_2 > \text{CS}_2 \gg \text{CO}$. The IR spectrum of **4** contains a medium-intensity band assigned to $\nu(\text{C-S})$ at 1010 cm^{-1} . This value agrees rather well with the complex $\text{Pt}_2(\mu\text{-CS}_2)\text{Cl}_2(\text{dppm})_2$,¹² which has one CS_2 band, $\nu(\text{CS}) = 985 \text{ cm}^{-1}$.

The 200-MHz ^1H NMR spectrum of **4** is considerably more complex than that of either **1**, **2**, or **3**. One methylene resonance is observed as a complex asymmetric eight-line multiplet at $\delta 2.40$, which apparently results from overlap of two different methylene signals. The $^{31}\text{P}\{^1\text{H}\}$ and $^{13}\text{C}\{^1\text{H}\}$ NMR data for **4** together are extremely informative with regard to the mode of bonding which CS_2 has adopted in **4**. The $^{31}\text{P}\{^1\text{H}\}$ NMR spectrum of **4** appears as an AA'BB' multiplet centered at $\delta -8.83$. The $^{13}\text{C}\{^1\text{H}\}$ NMR spectrum of **4** exhibits only one dmpm methylene signal at $\delta 28.0$ as a phosphorus-split triplet at 25°C . These results are consistent with maintenance of an asymmetrically bridged CS_2 ligand, while the dmpm methylene carbon atoms are equilibrated, presumably through flexing of the $\text{Pd}_2\text{P}_4\text{C}_2$ ring. The proposed structure for **4** is consistent with that observed for $\text{Pt}_2(\mu\text{-CS}_2)\text{Cl}_2(\text{dppm})_2$.¹² The electronic absorption spectrum of **4** does not reveal the isolated intense low-energy band characteristic of **2** and **3**. Instead, only a series of overlapped bands in the 300–400-nm region are observed.

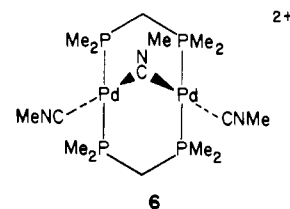


The reaction of **1** with 1 equiv of CH_3NC proceeds in a manner similar to the reaction with the other small molecules of this study. The resulting product, $\text{Pd}_2(\mu\text{-CNCH}_3)\text{Cl}_2(\text{dmpm})_2$ (**5**), is generally obtained in 75% yield as a yellow crystalline solid. Complex **5** is slightly air-sensitive as a solid. The IR spectrum of **5** in CH_2Cl_2 solution or as a solid shows only bands characteristic of a bridging isocyanide. In both solution and the solid state, however, two such bands appear. In the solid state these occur at 1675 and 1630 cm^{-1} . The weaker high-energy band can only be ascribed to a combination or overtone band. A similar interpretation has been advanced for dppm-bridged $\mu\text{-CNMe}$ complexes.⁵ The $^{31}\text{P}\{^1\text{H}\}$ NMR spectrum of **5** consists of a singlet at $\delta 1.50$, implying an approximately symmetrically bridged CH_3NC ligand on the NMR time scale. All other spectroscopic data for **5** are consistent with a $\mu\text{-CNCH}_3$ A-frame structure. The electronic spectrum of **5**



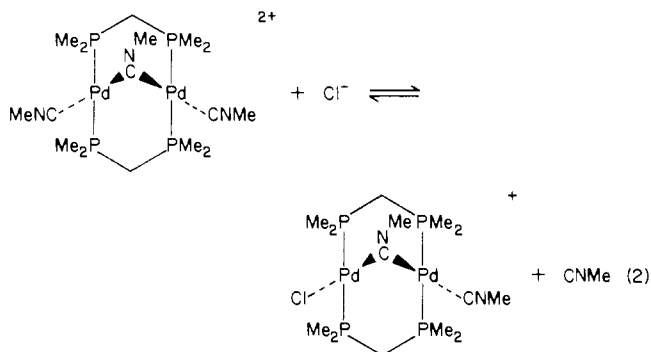
is similar to those of **2** and **3** in that it has a prominent intense low-energy band at $\lambda_{\text{max}} = 406 \text{ nm}$, which is responsible for the yellow color of the complex.

The reaction of **1** with excess CH_3NC proceeds quite differently from the reactions with CO , CS_2 , and SO_2 . When **1** is treated with at least 3 equiv of CH_3NC , a new material, **6**, can be obtained in 40% yield. Complex **6** readily loses CNCH_3 under vacuum. The IR spectrum of **6** reveals both bridging and terminal $\nu(\text{CN})$ bands at $2230, 1670, \text{ and } 1625 \text{ cm}^{-1}$. At 25°C , the 200-MHz ^1H NMR spectrum of **6** indicates one CH_3NC environment. At -80°C , two distinct CH_3NC signals easily can be discerned at $\delta 3.60$ and 3.27 , which integrate in the ratio 2:1. These data suggest that **6** possesses an A-frame structure with a single bridging CH_3NC ligand and two terminal CH_3NC ligands, and is thus analogous to the first dppm-bridged Pd A-frame complex, reported by Balch in 1977.⁵ An interesting distinction of the



dmpm-bridged complex **6** is that the terminal isocyanide ligands are quite labile in solution. Thus when **6**, as the chloride salt, is dissolved in solutions, free CH_3NC can be observed by IR and a new species, presumably $[\text{Pd}_2(\mu\text{-CNMe})(\text{CNMe})\text{Cl}(\text{dmpm})_2]^+$, can be identified spectroscopically. These observations suggest that the chloride salt of **6** is involved in a reversible equilibrium (eq 2). The increased lability of the terminal ligand positions in dmpm-bridged binuclear Pd complexes has been noted previously, particularly in studies of the water solubility of **1**.³ The labilized terminal ligand sites are apparently a consequence of the enhanced donor ability of the bridging dmpm ligands relative to dppm.

It is evident that there are general trends in the $^{31}\text{P}\{^1\text{H}\}$ NMR spectra of the new complexes reported above that have predictive value regarding the type of complex formed. Addition of small



molecules to the Pd–Pd bond results in a large downfield chemical shift of 20–40 ppm in $^{31}\text{P}\{\text{H}\}$ NMR spectra. The downfield shifts can be rationalized in terms of the electron-withdrawing nature of the bridgehead ligands. It is interesting to note that a relative ordering of the electrophilicity of the various bridgehead molecules can be made. Complex **3** is furthest downfield among the “A-frame” complexes while complex **4** is furthest upfield. This is consistent with the expectation that SO_2 is more electron-withdrawing than CS_2 . By comparing the $^{31}\text{P}\{\text{H}\}$ chemical shifts of the various complexes, one can obtain a relative ordering of bridgehead ligand electrophilicity: $\text{SO}_2 > \text{CO} > \text{CH}_3\text{NC} > \text{CS}_2$.

The electronic spectra of these complexes exhibit intense low-energy absorption bands. These bands are not present in the M–M-bonded species and are assigned to be Pd \rightarrow bridgehead ligand charge transfer. This assignment is based on similar data found in the $\text{Pt}_2(\text{dppm})_2(\text{SnCl}_3)_2$ ^{26,27} system in which an intense low-energy band at $\lambda_{\text{max}} = 505$ nm is found that is not present in $\text{Pt}_2(\text{dppm})_2\text{Cl}_2$ and is assigned to Pt to Sn charge transfer. We find an interesting trend between $^{31}\text{P}\{\text{H}\}$ NMR chemical shifts and λ_{max} of the low-energy bands in complexes **2–5**. Complex **3**, which exhibits the lowest energy absorption band in its electronic spectrum, also has the highest downfield chemical shift in the $^{31}\text{P}\{\text{H}\}$ spectrum. Complex **2** and **5** have similar ^{31}P chemical shifts and exhibit similar low-energy absorption bands in the 400–450-nm range. Complex **3** does not exhibit a well-defined low-energy band, in keeping with this complex's high upfield ^{31}P chemical shift. The d^9 – d^9 M–M-bonded M_2L_6 complexes have an electronic configuration in which only the σ^* orbital is vacant, leaving a $\sigma^2(\pi_1)^4(\pi_2)^4(\pi_1^*)^4(\pi_2^*)^4(\sigma^*)^0$ configuration.²⁷ In this

model, $d\pi^* \rightarrow \sigma^*$ is expected to be the lowest energy electronic transition. Insertion of a small molecule, L, into the M–M bond results in formation of “A-frame” type complexes. A new qualitative bonding scheme is then appropriate in which accessible π^* orbitals of the added bridgehead ligand are vacant, and as a consequence $\text{M}(d\pi^*) \rightarrow \text{L}(\pi^*)$ transitions may occur at lower energy than $d\pi^* \rightarrow \sigma^*$. Complex **3** then has the lowest apparent $\text{M}(d\pi^*) \rightarrow \text{L}(\pi^*)$ energy separation, as determined by its electronic spectrum. The apparent energies of the $\text{M}(d\pi^*) \rightarrow \text{L}(\pi^*)$ absorption bands for complexes **2–5** systematically increase in the order $3 < 2 < 5 < 4$ while $^{31}\text{P}\{\text{H}\}$ NMR chemical shifts of these complexes move to higher fields in the same order.

Conclusions

The complexes reported herein result from the insertion of small molecules, CO, CH_3NC , CS_2 , and SO_2 , into the Pd–Pd bond of dmpm-bridged dipalladium complexes. The X-ray structure of the CO adduct, **2**, reveals a characteristic “A-frame” type structure with the CO molecule bound symmetrically between the Pd centers. The separation of 3.171 (1) Å is consistent with the absence of a Pd–Pd bond. Reactions of **1** with CH_3NC , CS_2 , and SO_2 similarly proceed to form 1:1 adducts. The reaction with CH_3NC however proceeds further in the presence of excess ligand to replace both terminal chloride ligands.

The $^{31}\text{P}\{\text{H}\}$ NMR spectra of the 1:1 complexes all exhibit signals of 20–40 ppm downfield of **1**. The degree of the downfield $^{31}\text{P}\{\text{H}\}$ chemical shift qualitatively follows the electrophilicity of the added small molecule in the order $\text{SO}_2 > \text{CO} > \text{CH}_3\text{NC} > \text{CS}_2$. The $^{31}\text{P}\{\text{H}\}$ chemical shifts of **2–5** also correlate with the energy of the lowest energy charge-transfer absorption band in the UV–vis electronic absorption spectra of these complexes.

Acknowledgment. This work was supported by the National Science Foundation (Grant CHE-8411836) and the U.S. Department of Energy (Grant DE-FG22-84PL70791). Additional support from Stauffer Chemical Co. is gratefully acknowledged. M.L.K. wishes to acknowledge David Ross and Chevron Fellowships. The PDP 11/34 computer and X-ray structure solution package of the Department of Chemistry were purchased with funds from the NSF Chemical Instrumentation Program (Grant CHE-8204994) and the Monsanto Fund. A generous loan of PdCl_2 from Johnson Matthey, Inc., is appreciated.

Supplementary Material Available: Tables of general temperature factor expressions, torsion angles, observed and calculated structure factors, and bonding and selected nonbonding distances and bond angles for $\text{Pd}_2(\mu\text{-CO})\text{Cl}_2(\text{dmpm})_2$ and a discussion of ^1H , $^{13}\text{C}\{\text{H}\}$, and $^{31}\text{P}\{\text{H}\}$ NMR data (28 pages). Ordering information is given on any current masthead page.

(26) Garciafigueroa, E.; Sourisseau, C. *Nouv. J. Chim.* **1978**, *2*, 593.

(27) Alves, O. L.; Vitorge, M. C.; Sourisseau, C. *Nouv. J. Chim.* **1983**, *7*, 231.